Surface Chemistry

DOI: 10.1002/ange.201301580

Identification of Molecular-Adsorption Geometries and Intermolecular Hydrogen-Bonding Configurations by In Situ STM Manipulation**

Wei Xu, Huihui Kong, Chi Zhang, Qiang Sun, Henkjan Gersen, Liang Dong, Qinggang Tan, Erik Lægsgaard, and Flemming Besenbacher**

The direct recognition[1–7] and controllable transformation[8,9] of the molecular-adsorption geometries of self-assembled surface nanostructures has shown significant potential for the miniaturization of functional devices and is one of the challenging goals within the field of nanoscience and nanotechnology. Manipulation by scanning tunneling microscopy (STM) provides the surface-science community with a direct approach to induce a variety of molecular motions, such as isomerization,[10,11] rotation,[12–14] and translation[15,16] on surfaces, and moreover to characterize intermolecular forces[17,18] and molecular configurations.[11,19] Studies reported in these areas have so far been mainly focused on single-molecule phenomena, and in most cases, for example, the isomerization of azobenzene and its derivatives, the switch is to some degree stochastic. However, the manipulation of larger structural motifs with precise control and the further identification of intermolecular interactions at the single-molecule scale have little been reported to date. It is therefore of particular interest to extend the STM manipulation technique to more complex situations to gain further insight into the direct identification and controllable regulation of intermolecular interactions and molecule–substrate interactions in general towards the fabrication of desired nanostructures on surfaces.

[*] Prof. Dr. W. Xu, H. Kong, C. Zhang, Q. Sun, L. Dong, Prof. Dr. Q. Tan
College of Materials Science and Engineering, Key Laboratory for Advanced Civil Engineering Materials (Ministry of Education)
Tongji University
Caoan Road 4800, Shanghai 201804 (P.R. China)
E-mail: xuwei@tongji.edu.cn

Prof. Dr. W. Xu, Prof. E. Lægsgaard, Prof. Dr. F. Besenbacher
Interdisciplinary Nanoscience Center (iNANO) and
Department of Physics and Astronomy, Aarhus University
DK 8000 Aarhus C (Denmark)
E-mail: fbe@inano.au.dk

H. Gersen
Nanophysics and Soft Matter Group
H. H. Wills Physics Laboratory, University of Bristol
Tyndal Avenue, BS8 1TL, Bristol (UK)

[**] We acknowledge financial support from the Danish Ministry for Science, Technology and Innovation, the Danish Research Councils, the Danish National Research Foundation, The Carlsberg Foundation, the Villum Kahn Rasmussen Foundation, the ERC (through an advanced grant (FB)), The National Natural Science Foundation of China (21103128), the Program for New Century Excellent Talents in University (NCET-09-0607), the Shanghai Pujiang Program (11PJ1409700), the Shanghai "Shu Guang" Project (11SG25), and the Fundamental Research Funds for the Central Universities.

STM = scanning tunneling microscopy.

Supporting information for this article is available on the WWW under http://dx.doi.org/10.1002/anie.201301580.

Herein, we investigate the adsorption and self-assembly of a photochromic oxazine molecule on a Cu(110) surface by STM imaging and in situ manipulation under ultrahigh-vacuum (UHV) conditions and density functional theory (DFT) calculations. STM imaging revealed that the molecules could form either dim stripes or bright clusters upon the thermally induced ring opening[20] of the molecule (Figure 1a). From calculated models, we identified three distinct hydrogen-bonding configurations involved in the dim-dimer and bright-dimer/tetramer structural motifs that serve as the building blocks for the dim-stripe and bright-cluster structures. Surprisingly, by in situ STM manipulation we could controllably switch the different hydrogen-bonding configurations within these three structural motifs at room temperature. The results demonstrate that in situ STM manipulation could be employed as a direct approach to probe larger structural motifs, in which molecular-adsorption geometries and intermolecular bonding configurations could be identified at the single-molecule scale. This method may also be extended to other surface supramolecular systems to supplement qualitative understanding of intermolecular interactions on the basis of STM results.

After deposition of the oxazine molecules on Cu(110) held at room temperature, we found that most of the molecules were randomly distributed on the surface (see Figure S1 in the Supporting Information). However, if we annealed the surface slightly (ca. 400 K) right after deposition of the molecules at a low coverage (ca. 0.1 monolayer), two kinds of distinct self-assembled nanostructures (dim molecular stripes and bright molecular clusters) were revealed by STM (Figure 1b). The dim and bright species appeared to have different heights (by 0.7 Å; see the line profile for the STM image in Figure 1c). As shown in the STM image, the dim stripes consist of dimers as the elementary structural motif, and the bright clusters are mainly composed of monomers, dimers, and tetramers (the corresponding close-up STM images are shown in Figure 2). From the close-up STM images, we could identify that within the bright tetramer, the two molecules along the short diagonal of the rhombus shape were apparently smaller than the other two. Since these self-assembled dim and bright nanostructures are clearly different from the structure before annealing, and since, according to the previous studies,[9,20] the on-surface ring-opening reaction of molecules of this type is completely triggered as soon as the anneal temperature reaches 330 K, we believe that both the dim and the bright structures are formed by the open-form molecules. Thus, the question as to what factors induce the observed differences in the apparent height and size of the molecules arises. As the dim species always

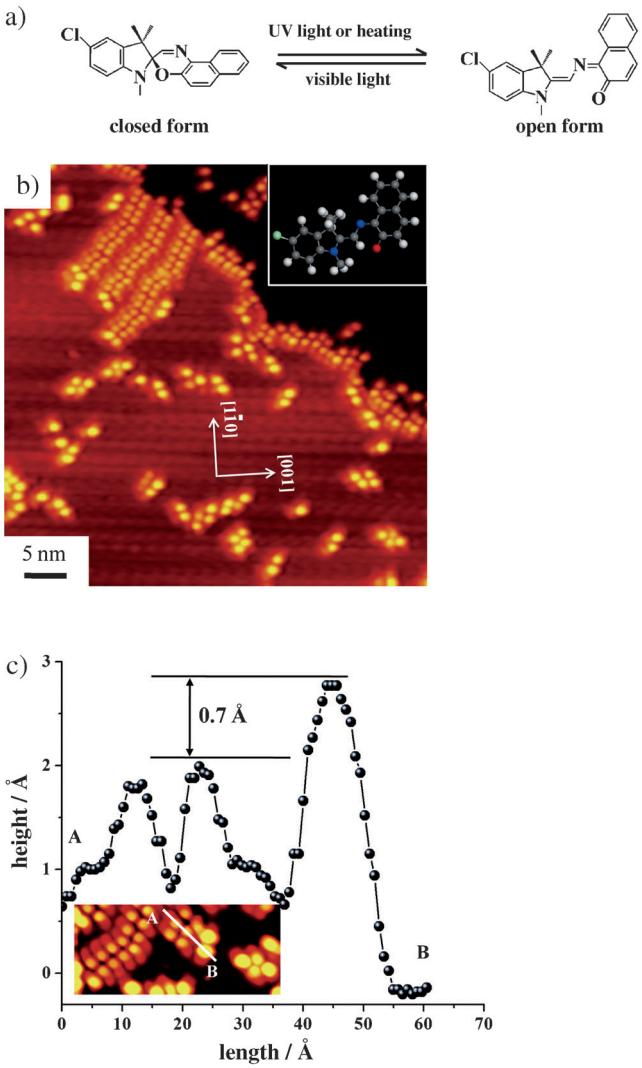

Figure 1. a) Interconversion of a photochromic oxazine molecule between the closed form and the open form. b) STM image showing two kinds of distinct nanostructures (dim stripes and bright clusters) with different apparent heights formed by the open-form molecules. The lattice direction of the Cu(110) surface is indicated in the image. Scanning conditions: $I_t = 0.58$ nA, $V_t = -1486$ mV. c) Line profile across dim and bright species. A difference in height of 0.7 Å was found.

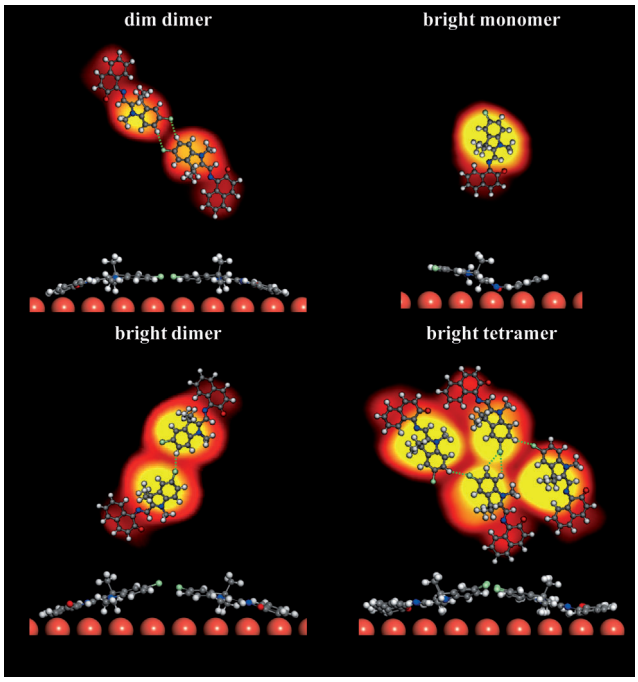

Figure 2. High-resolution STM images and calculated models of the three typical structural motifs and the single molecule. In each case, the top view of the calculated model structure is superimposed on the corresponding STM image, and the side-view model is shown below. Scanning conditions: $I_t = 0.58$ nA, $V_t = -1486$ mV.

exist in the dimer form in the stripes (no monomers were found), and the bright smaller molecules could only be found within the tetramer structure and did not exist as monomers or in the bright-dimer form, we speculate that the specific intermolecular interactions involved in these structural motifs must be the main reason responsible for the observed differences in apparent height and size.

To unravel the mystery and gain atomic-scale insight into these structural motifs, we performed detailed DFT calculations on a variety of dimer/tetramer structures involving the copper substrate. Superposition of the most stable relaxed models of the dim-dimer, bright-monomer, bright-dimer, and bright-tetramer structures on the corresponding close-up STM images demonstrated good agreement (Figure 2). It can be seen from the top-view model (for clear presentation, the underlying copper surface was omitted) that the dim-dimer motif is a homochiral structure that adopts a head-to-head double C–H···Cl hydrogen-bonding configuration. For the bright monomer, two enantiomers exist on the surface; however, the enantiomers have the same adsorption energy and cannot be distinguished from STM images. In contrast with the dim dimer, the bright-dimer motif is a heterochiral structure that adopts a head-to-head single C–H···Cl hydrogen-bonding configuration. When two bright dimers join together, two new C–H···Cl hydrogen bonds form (two hydrogen-donor C–H groups share one Cl atom) to link the dimers; thus, a new hydrogen-bonding configuration induces the formation of the bright tetramer. In this way, we identified three different hydrogen-bonding configurations in total in the above-mentioned structural motifs. Analysis of the side-view models shown in Figure 2 showed that different hydrogen-bonding configurations could indeed induce different molecular-adsorption geometries. These different molecular-adsorption geometries are very likely responsible for the observed differences in the apparent height and size of the molecules.

To explore the possibility of switching between different hydrogen-bonding configurations within the structural motifs, we performed a series of in situ STM manipulations at room temperature. The lateral manipulations were carried out in a controllable line-scan mode under specific scanning conditions (by increasing the tunnel current up to approximately 2.0 nA while reducing the tunnel voltage down to approximately 20 mV[14,15]). Figure 3 a–d shows that the manipulation of two adjacent dim dimers (those underneath the green

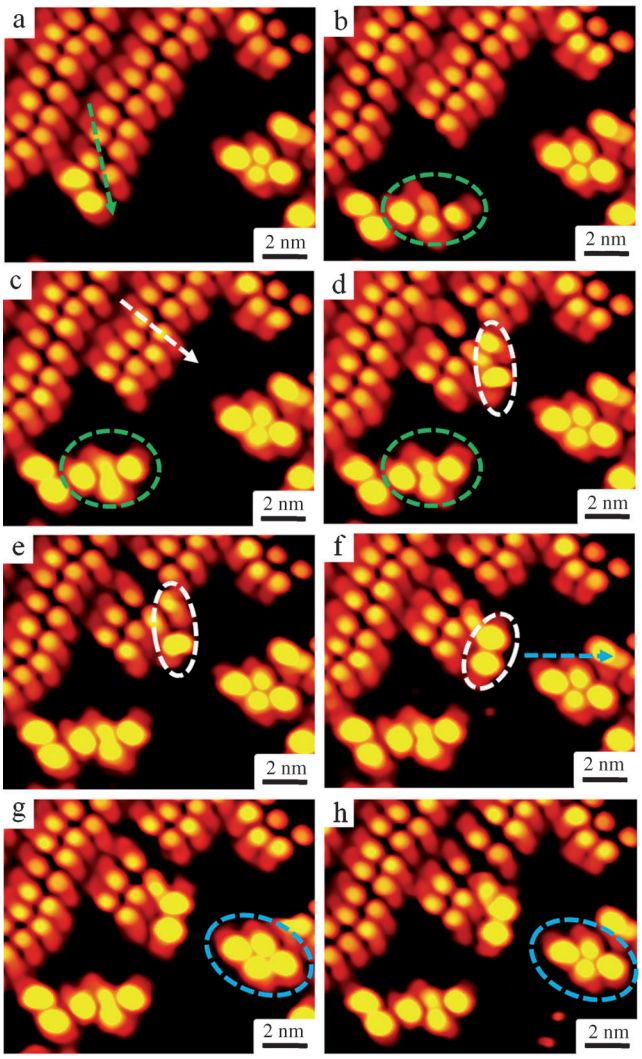

Figure 3. Lateral STM manipulations demonstrating controllable switching among three structural motifs shown in Figure 2. a–d) Conversion of two adjacent dim dimers into a bright tetramer. The green arrow in (a) indicates the location and direction of the manipulation applied, and the green ellipses in (b–d) highlight the configurational evolution into a bright tetramer. c–f) Conversion of one dim dimer into a bright dimer. The white arrow in (c) indicates the location and direction of the manipulation applied, and the white ellipses in (d–f) highlight the configurational evolution into a bright dimer. f–h) Conversion of the two smaller molecules along the short diagonal within a bright tetramer into two larger molecules, and the spontaneous transformation back into two smaller molecules during the next scanning process. The blue arrow in (f) shows the direction of the manipulation applied, and the blue ellipses highlight the configurational evolution into two bright dimers (g) and then back into a tetramer (h). Scanning conditions: $I_t = 0.54$ nA, $V_t = -1400$ mV; manipulation conditions: $I_t = 2.0$ nA, $V_t = 20$ mV.

arrow, which shows the direction of manipulation, in Figure 3a) resulted in the disassociation of the dim dimers from the molecular stripe and the formation of a tetramer-like structure consisting of three bright molecules and a dim molecule (those within the green ellipse in Figure 3b). Interestingly, when we continued scanning, this tetramer-like structure spontaneously evolved into the typical bright-tetramer motif discussed above (indicated by the green ellipse in Figure 3c,d). Such lateral manipulation was also performed on an individual dim dimer located in the middle of a stripe (the dimer underneath the white arrow, which shows the direction of manipulation, in Figure 3c). Upon manipulation (Figure 3d–f), this dim dimer was first detached from the stripe and converted into two bright molecules (indicated by the white ellipse in Figure 3d), which then spontaneously evolved into the typical bright-dimer motif (see the white ellipses in Figure 3e,f). From the above findings, we could draw the following conclusions: 1) Cleavage of the dim-dimer motif is the prerequisite for initiation of the switching process. 2) Once the dim dimer has been cleaved, the separated dim molecules can then be converted into bright molecules, and the bright molecules can spontaneously evolve into the typical bright-dimer/tetramer motifs in a further step. The bright molecules, however, cannot be switched to dim molecules by such lateral manipulation (not shown). 3) Switching from the dim dimer to the bright dimer/tetramer indicates successful conversion of the hydrogen-bonding configurations within the structural motifs.

We also attempted to manipulate the bright-tetramer motif (Figure 3 f–h). Surprisingly, after several trials, a delicate manipulation (in the direction of the blue arrow in Figure 3 f) enabled the intermolecular bonding configurations within the tetramer motif to be switched in situ, so that the two smaller molecules along the short diagonal of the tetramer became larger (see the blue ellipse in Figure 3g). This result indicated the cleavage of the hydrogen bonds that linked the two bright dimers. However, during the next scanning process, we found that the two bright dimers reformed the bright tetramer (see the blue ellipse in Figure 3h). Thus, we could conclude that the hydrogen bonds between the two bright dimers were reformed, which strongly indicates that the difference in the apparent size of the molecules within the bright-tetramer motif is induced by the specific hydrogen-bonding configurations.

In conclusion, from a combination of high-resolution STM imaging/delicate lateral manipulation and DFT calculations we have identified three molecular structural motifs with distinct hydrogen-bonding configurations formed by the open-form oxazine molecules on Cu(110). The different intermolecular hydrogen-bonding configurations, which result in different molecular-adsorption geometries, were revealed to be responsible for the observed differences in the apparent height and size of molecules within the structural motifs. STM manipulations proved to be a powerful tool for directly probing molecular-adsorption geometries and moreover for the controllable switching of the intermolecular hydrogen-bonding configurations involved in the structural motifs. These findings demonstrate how STM manipulation could be extended from triggering of various on-surface motions to probing of the intermolecular bonding modes in self-assembled nanostructures. An understanding of such bonding modes can provide fundamental insight into distinct intermolecular interactions and is thus of utmost importance from an experimental viewpoint.

Received: February 23, 2013
Revised: April 29, 2013
Published online: June 4, 2013

Keywords: density functional calculations · hydrogen bonds · intermolecular interactions · nanostructures · scanning tunneling microscopy

[1] T. Huang, Z. P. Hu, A. D. Zhao, H. Q. Wang, B. Wang, J. L. Yang, J. G. Hou, *J. Am. Chem. Soc.* **2007**, *129*, 3857.
[2] P. Messina, A. Dmitriev, N. Lin, H. Spillmann, M. Abel, J. V. Barth, K. Kern, *J. Am. Chem. Soc.* **2002**, *124*, 14000.
[3] A. Kühnle, T. R. Linderoth, B. Hammer, F. Besenbacher, *Nature* **2002**, *415*, 891.
[4] W. Xu, M. D. Dong, H. Gersen, E. Rauls, S. Vázquez-Campos, M. Crego-Calama, D. N. Reinhoudt, I. Stensgaard, E. Laegsgaard, T. R. Linderoth, F. Besenbacher, *Small* **2007**, *3*, 854.
[5] Y. Wang, M. Lingenfelder, T. Classen, G. Costantini, K. Kern, *J. Am. Chem. Soc.* **2007**, *129*, 15742.
[6] R. Otero, W. Xu, M. Lukas, R. E. A. Kelly, E. Laegsgaard, I. Stensgaard, J. Kjems, L. N. Kantorovich, F. Besenbacher, *Angew. Chem.* **2008**, *120*, 9819; *Angew. Chem. Int. Ed.* **2008**, *47*, 9673.
[7] W. Xu, J. G. Wang, M. F. Jacobsen, M. Mura, M. Yu, R. E. A. Kelly, Q. Q. Meng, E. Laegsgaard, I. Stensgaard, T. R. Linderoth, J. Kjems, L. N. Kantorovich, K. V. Gothelf, F. Besenbacher, *Angew. Chem.* **2010**, *122*, 9563; *Angew. Chem. Int. Ed.* **2010**, *49*, 9373.
[8] J. Mielke, F. Leyssner, M. Koch, S. Meyer, Y. Luo, S. Selvanathan, R. Haag, P. Tegeder, L. Grill, *ACS Nano* **2011**, *5*, 2090.
[9] M. Piantek, G. Schulze, M. Koch, K. J. Franke, F. Leyssner, A. Krüger, C. Navío, J. Miguel, M. Bernien, M. Wolf, W. Kuch, P. Tegeder, J. I. Pascual, *J. Am. Chem. Soc.* **2009**, *131*, 12729.
[10] A. Safiei, J. Henzl, K. Morgenstern, *Phys. Rev. Lett.* **2010**, *104*, 216102.
[11] M. Alemani, M. V. Peters, S. Hecht, K. H. Rieder, F. Moresco, L. Grill, *J. Am. Chem. Soc.* **2006**, *128*, 14446.
[12] L. Grill, K. H. Rieder, F. Moresco, G. Rapenne, S. Stojkovic, X. Bouju, C. Joachim, *Nat. Nanotechnol.* **2007**, *2*, 95.
[13] N. Wintjes, D. Bonifazi, F. Y. Cheng, A. Kiebele, M. Stohr, T. Jung, H. Spillmann, F. Diederich, *Angew. Chem.* **2007**, *119*, 4167; *Angew. Chem. Int. Ed.* **2007**, *46*, 4089.
[14] M. Yu, W. Xu, Y. Benjalal, R. Barattin, E. Laegsgaard, I. Stensgaard, M. Hliwa, X. Bouju, A. Gourdon, C. Joachim, T. R. Linderoth, F. Besenbacher, *Nano Res.* **2009**, *2*, 254.
[15] F. Rosei, M. Schunack, P. Jiang, A. Gourdon, E. Laegsgaard, I. Stensgaard, C. Joachim, F. Besenbacher, *Science* **2002**, *296*, 328.
[16] Y. Shirai, A. J. Osgood, Y. M. Zhao, K. F. Kelly, J. M. Tour, *Nano Lett.* **2005**, *5*, 2330.
[17] L. Grill, M. Dyer, L. Lafferentz, M. Persson, M. V. Peters, S. Hecht, *Nat. Nanotechnol.* **2007**, *2*, 687.
[18] W. Xu, R. E. A. Kelly, R. Otero, M. Schöck, E. Laegsgaard, I. Stensgaard, L. N. Kantorovich, F. Besenbacher, *Small* **2007**, *3*, 2011.
[19] J. Henzl, M. Mehlhorn, H. Gawronski, K. H. Rieder, K. Morgenstern, *Angew. Chem.* **2006**, *118*, 617; *Angew. Chem. Int. Ed.* **2006**, *45*, 603.
[20] C. Bronner, G. Schulze, K. J. Franke, J. I. Pascual, P. Tegeder, *J. Phys. Condens. Matter* **2011**, *23*, 484005.

